Enhancing Heat Transfer of Drag Reducing Surfactant Solutions with Static Mixers

Thesis

Presented in Partial Fulfillment of the Requirements for the Bachelor of Science with Honors Research Distinction in Chemical Engineering, The Ohio State University

By

Stiphany Tieu

Department of Chemical and Biomolecular Engineering

The Ohio State University

2019

Honors Examination Committee:

Andrew J. Maxson, Advisor

James F. Rathman

Abstract

At very low concentrations (in parts per million or ppm), surfactant drag reducing solutions have been shown to significantly reduce the pressure drop in turbulent flow systems. These solutions are of interest in industry because they can lower the pumping energy requirements and subsequently, costs, in recirculating flow systems. Unfortunately, drag reduction (DR) is coupled with heat transfer reduction (HTR), which is undesirable for commercial applications like district heating and cooling (DHC) systems because it renders the technology uneconomical. Thus, many methods, including ultrasonication and photosensitive counterions, have been developed and used to improve heat transfer in surfactant DR solutions. Many of these methods are complicated, expensive to implement, require high energy inputs, or result in high pressure drop penalties. Static mixers, however, are simple and easily installed into heat exchangers, so manufacturers can retrofit existing tubes. In this study, four static mixers were constructed by attaching three-dimensional printed elements with 45 degree pitch onto 48-inch carbon fiber rods with the following designs: one blade, two blades spaced one-fourth and three-fourth of the way of the heat exchanger tube, two blades spaced one-third and two-third of the way of the tube, and three blades spaced evenly. These showed significant improvement of heat transfer when tested with varying positions in the heat exchanger in the recirculating flow system.

This is dedicated to Dwight, my wiener dog.

Acknowledgments

Although I did not know Prof. Zakin well, I am deeply grateful for the opportunity to pursue this research and learn about turbulent drag reduction. I would like to thank Dr. Andy Maxson in the William G. Lowrie Department of Chemical and Biomolecular Engineering for sharing wisdom, support, and encouragement. His random visits to "zoo exhibit" in the unit ops lab, wild conspiracy theories, and pictures of his kids were always enjoyable. I also take this opportunity to express immense gratitude and appreciation to Ross Chongson for his mentorship, support, and love for dogs. I would also like to thank Prof. Rathman for his sincere and valuable kindness and guidance over the years.

I am filled with gratitude for Brian and Wenda. My success in my undergraduate career would not be possible without their support.

I thank my boyfriend, Najeeb, for encouraging and feeding me. Also, shout out to Leah and the boys of 2136 for helping me keep my sanity. Finally, I would like to express appreciation the students in Dr. Maxson's turbulent drag reduction lab, John and Jon, for their help and friendship.

Contents

List of Tables

Table **Page**

List of Figures

Chapter 1: Introduction

1.1 History

Drag reduction (DR) is the phenomenon observed when the introduction of an additive to turbulent flow results in a reduction of friction pressure loss. DR lowers the pumping energy requirement of flow systems, allows for reduced pipe diameters, and increases flow rates while holding pressure constant [8]. These advantages lead to decreased maintenance and operating costs.

Examples of additives that can achieve this DR effect include high molecular weight polymers, fibers, aluminum disoaps, and surfactants [9]. Certain drag reducing additives (DRAs), such as high molecular weight polymers, degrade with shearing [2]. Shear degradation sources include pumps and constrictions. This degradation renders high molecular weight polymer solutions ineffective in regards to DR. As a result, these polymer DR solutions can either only be used once, or they must be continually replenished in the system. These factors limit the practicality of polymer solutions for application in recirculation systems.

1.2 Surfactant drag reducing additives

Unlike high molecular weight polymers, surfactant DRAs are able to self-assemble quickly. Surfactants, also known as surface-active agents, form wormlike micelles (WLMs) that are able to reassemble within seconds [5]. The WLMs break up with exposure to high shear, but they reassemble and become effective DRAs again. This makes surfactant DRAs suitable for application in recirculating flow systems, such as district heating and cooling (DHC) systems.

1.3 Heat transfer reduction

Alas, DR is coupled with heat transfer reduction (HTR). The HTR phenomenon observed in these flow systems is not fully understood, but it has been attributed to the increase of the viscous sublayer thickness [7] and decrease in turbulence intensities in the radial and tangential directions [3]. HTR is undesirable in recirculating heat transport systems, such as DHCs, because it renders the heat transfer (HT) fluids significantly less effective. Although DR reduces the pumping energy requirements in these turbulent flow systems, the HTR is generally always higher [1].

1.4 Application in district heating and cooling systems

In DHC systems, water is heated or cooled in a centralized location and pumped to nearby buildings to regulate temperature. DHCs provide energy-efficient and cost-effective solutions in the climate control market. Taking into consideration the enviro-economic function of DHC systems, it can be concluded these are more efficient than individual heating and cooling units. Policies are focused to shift the primary energy

source to DHC systems, which are open to research for improvements to the technology [4]. A major limitation of these heat transportation systems is the high pumping energy requirements to move the HT fluid across long distances. The application of surfactant DR solutions to DHC systems has been a popular area of research because of the pumping energy savings. It was shown that a few hundred ppm of surfactant in the Kawaguchi's flow system saved 70% of the pumping power [10]. However, the HT must be improved to make this technology feasible. The effectiveness and efficiency of the HT fluids are crucial to DHC systems, so optimizing the configuration of the static mixer to enhance heat transfer can be explored to improve the application of surfactant DR solutions in these heat transportation systems.

1.5 Overview of research

Introducing a static mixer in the heat exchanger is expected to improve HT in the turbulent, recirculating flow system via bulk mixing. The blades will disrupt the thermal boundary layer, allow the warmer fluid on the conduit walls to propagate to the center, and make the temperature profile more uniform. In these experiments, the DR, HTR, and pressure drop data for surfactant DR solutions with and without the static mixers will be collected and analyzed.

It is hypothesized the HTR will be as low as 25% with the static mixer with three blades. Improving the heat transfer in these turbulent flow systems could suggest that surfactant DR solutions have practical application in heat transportation systems.

Chapter 2: Literature Review

2.1 Introduction

Surfactant drag reducing solutions can be applied to district heating and cooling (DHC) systems to provide pumping energy savings. However, there is hesitation in using surfactant DRAs in some systems due to the HTR associated with them. In response, there has been and continues to be interest in conducting research to improve the heat transfer ability of surfactant DR solutions.

Heat transfer enhancement of these solutions can be achieved by reducing or eliminating the DR ability or by changing the flow structure with modifications to the geometry of the conduit walls of the heat exchanger [5]. Many approaches using these methods have been investigated and are discussed in this chapter.

2.2 Destruction of surfactant wormlike micelle structures

Several methods to directly improve the heat transfer of surfactant DR solutions involve destroying the WLMs at the heat exchanger entrance. The destruction of WLMs causes the surfactant solution to lose its DR ability, resulting in temporary heat transfer behavior similar to that of water as the solution moves through part of the heat exchanger. Downstream, the WLM nanostructures re-assemble to restore the DR ability of the solution.

Criteria for assessing the effectiveness of these destructive methods include the ability to disrupt the WLMs and the recovery of the nanostructures. These criteria are difficult to evaluate due to the lack of understanding of the DR mechanisms. It is not fully understood what role WLMs have in DR.

2.2.1 Ultrasonication

The effect of ultrasonic exposure on surfactant DR solutions was investigated by Qi et al. [5]. Ultrasonication disrupted the WLMs, reducing the DR effect and improving the solution's heat transfer ability. With 300 seconds of exposure, the HTR decreased from 82% to 24%. Although ultrasonication effectively enhanced the heat transfer, the energy input was too high to justify this technology.

2.2.2 Photosensitive counterions

The formation of the WLMs occurs because of the polar surfactant head groups' affinity for polar solvent and the fatty surfactant tails' affinity for each other [5]. Although not fully understood, it is hypothesized WLMs are important in imparting the DR effect. In cationic surfactant drag reducing solutions, the positively charged head groups are near each other. When a certain amount of counterion is added to the surfactant solution, charge screening between the head groups forms the WLMs. Photosensitive counterions create an opportunity for heat transfer enhancement by changing the configuration of the counterions in the heat exchanger.

In a study by Shi et al., irradiation with ultraviolet (UV) light caused the light responsive counterion to switch its configuration from *trans* to *cis* [8]. In the *trans* configuration, the counterion is an effective drag reducer. However, the solution loses its DR ability in the *cis* configuration. Therefore, irradiation with UV light can

be used to switch the counterion configuration before the solution enters the heat exchanger to reduce the DR ability and restore some heat transfer ability. Then, the configuration can be reversed with visible light exposure after the HT section to restore the DR behavior. This technique is depicted in Figure 2.1.

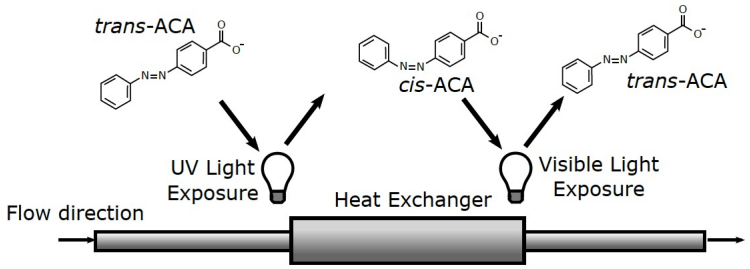

Figure 2.1: Switchable drag reduction with photosensitive counterions by A.M. 2017 [5].

The method of using photosensitive counterions was determined to be unsuitable for large scale applications due to its high cost and complexity [5]. This scheme would require installing exceptionally high intensity light sources on both sides of the heat exchanger.

2.3 Honeycombs, turbulators, and static mixers

Mechanical methods to improve heat transfer include installing honeycombs, static mixers, and turbulators into the heat exchanger [5]. These disrupt the WLMs prior to entering the heat exchanger tube, which causes the DR solution to behave like a Newtonian fluid with larger heat transfer coefficients [6]. In a study by Qi et al.,

honeycombs inserted at the entrance of heat exchanger tubes were determined to not have a significant effect on HTR [6]. Examples of turbulators include twisted-tapes and meshes. These can break or reduce the insulating boundary layer near the conduit surface, resulting in a higher heat transfer coefficient for the DR solution. However, turbulators result in large pressure losses [5]. Static mixers are simple and easier to retrofit heat exchangers with, thus demonstrating potential to be a more convenient method to improve heat transfer in DHC systems. An alternating helix static mixer design is shown in Figure 2.2.

Figure 2.2: Alternating helix mixer by A.M. 2017 [5].

This static mixer design was determined to be impractical because of its inefficiency and high pressure losses.

2.4 Modification of turbulent structure

Another approach to enhance heat transfer in surfactant DR solutions involves modifying the wall boundary layer and/or stimulating the turbulence intensity in the radial direction [5]. Previous studies using this approach can be found below.

2.4.1 High efficiency vortex

In studies by Shi, et al., high efficiency vortex (HEV) static mixers were used to enhance the radial turbulence intensity to improve heat transfer. The axial and tangential turbulence intensities were maintained to minimize the pressure drop penalty [5]. The HEV design has tabs inclined at a 30° angle on the conduit surfaces and is shown in Figure 2.4.1.

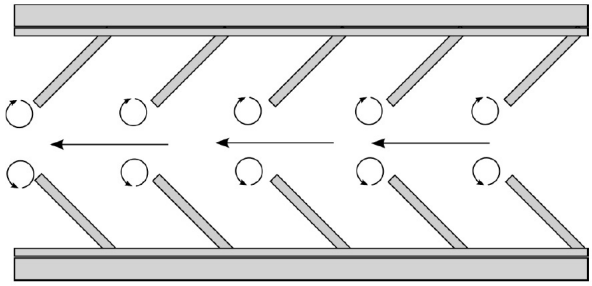

Figure 2.3: HEV design by A.M. 2017 [5].

2.4.2 Agitated heat exchangers

Maxson et al. explored the effects of using rotating agitators to enhance heat transfer in DR solutions. The agitator designs, which are shown in Figure 2.4.2, were based on common scraped surface heat exchangers (SSHEs) and installed into the heat exchanger. An external motor was run to rotate the agitators, which reduced HTR more than any previous heat transfer enhancement method for DR solutions without any measurable pressure losses [5]. However, the high power consumption by the external motor renders the technology impractical for large scale applications.

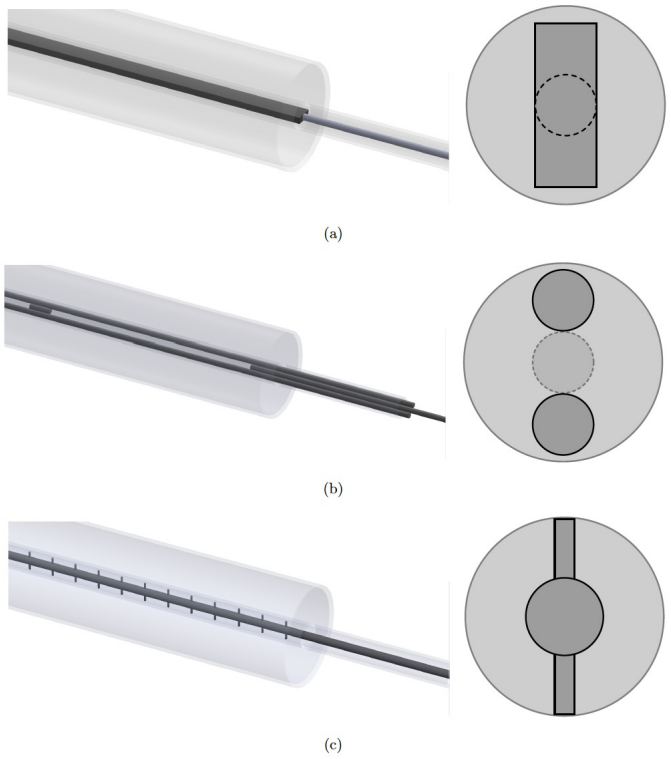

Figure 2.4: Three-dimensional representation of agitator designs by A.M. 2017 [5].

2.5 Conclusion

Although surfactant drag reducing solutions can create pumping energy savings for district heating and cooling systems, the reduced heat transfer ability does not justify their application in some systems. Methods to enhance the heat transfer in turbulent flow systems include the destruction of WLMs in the heat exchanger followed by downstream reassembly of the WLMs and heat exchanger designs that modify the turbulent structure in the tubes. Several past studies were discussed in this chapter. Many of them significantly improved the heat transfer in these surfactant DR systems. However, previous studies have disadvantages, including large pressure

drop penalties, high energy inputs, and complicated and expensive implementations. More research must be completed to determine more practical and energy efficient methods to improve heat transfer while maintaining the DR ability and minimizing the pressure drop. Limited previous work has been completed to improve the design of static mixers to achieve better heat transfer with minimized pressure loss. As such, this study will focus on testing different static mixer designs.

Chapter 3: Methodology

3.1 Recirculating flow system

The recirculating flow system was set up in the Ohio State University's unit operations laboratory to perform the static mixer experiments. This system was based on that from Maxson's experiments, which was originally described by Qi [5]. The general process flow diagram (PFD) of the system is shown in Figure 3.1.

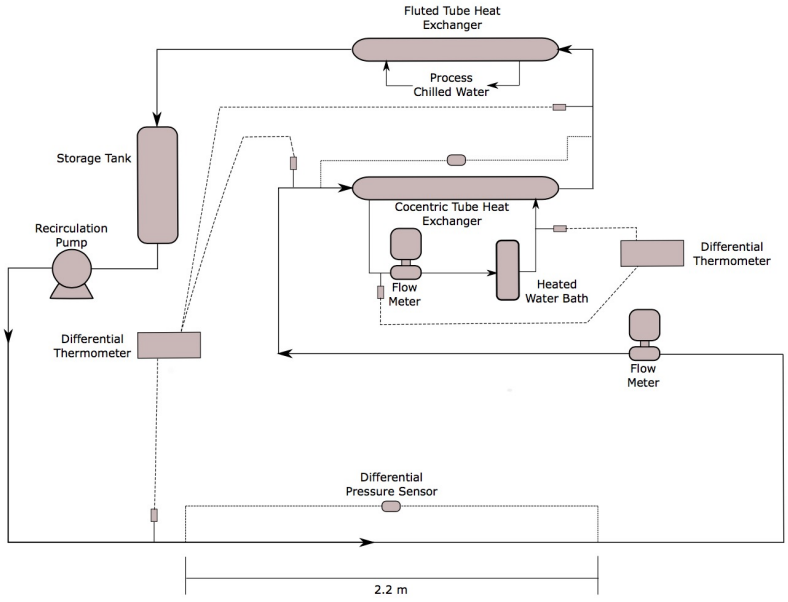

Figure 3.1: Schematic of recirculating flow system by R.C. 2019.

The system had an overall length of 24 m. The stainless steel tubing from the system had inner and outer diameters of 10.2 mm and 12.7 mm, respectively. It included a 0-10 psi Omega PX2300-10DI differential pressure transducer for DR pressure drop measurements and a 0-100 psi Omega PX2300-100DI differential pressure transducer to measure the pressure drop across the heat exchanger. There were four pressure taps. An Oberdorfer N7000S15 gear pump was used to recirculate the test solutions in the flow system.

The concentric tube heat exchanger was stainless steel, 36 inches in length, and insulated with 2-inch thick fiberglass pipe insulation. The inner and outer diameters of the inner tube were 10.2 mm and 12.7 mm, respectively, and the outer tube's diameter was 50 mm.

The recirculating flow loop begins with the cylindrical, stainless steel storage tank, which had a maximum capacity of 12 L. From here, the fluid is pumped to the DR section, where the differential pressure was measured across this 2.2 m pressure drop test section. Measurements were recorded with an Omega DaqBoard 2000 data acquisition system, and the data were collected in a Microsoft Excel spreadsheet. The spreadsheet uses a Modbus protocol to grab bits that are translated with calibrations to obtain meaningful pressure values. The test solution passes through the concentric tube heat exchanger with a countercurrent configuration, where hot water is supplied to the annulus of the heat exchanger by an 800 W NESLAB RTE-111 heated water bath and a VWR 1120 immersion circulator. Then, the test solution passes through a fluted tube heat exchanger, where cooling water flows through the shell to maintain a steady temperature as the solution returns to the storage tank. The flow rate of

the cooling water was controlled with a needle valve to maintain the desired inlet temperature on the tube-side of the fluted tube heat exchanger.

Two Physitemp BAT-10 multipurpose thermometers with Type T thermocouples were used to measure the temperature at the entrance to the DR pressure drop test section as well as the inlet and outlet temperatures of the shell- and tube-sides of the concentric tube heat exchanger. The latter four temperatures were used to determine the temperature differentials across the shell- and tube-side streams of the heat exchanger. The shell-side inlet temperature was kept at 50.0 °C, and the tube-side inlet temperature was maintained between 25.0 ° and 26.0 °C. The flow rate of the heated water on the shell-side of the concentric tube heat exchanger was maintained at 2.00 gpm with a ball valve. Manufacturer specifications report an accuracy of ± 0.01 °C and ± 0.1 °C for the differential temperature mode and single temperature mode, respectively. When the system and temperatures reached steady state, the thermometers were switched to the differential mode. Readings were recorded for both the shell- and tube-side streams. When the readings on the BAT-10 thermometers fluctuated, an average of the minimum and maximum values after observing for 30 seconds was taken.

Toshiba LF-404 electromagnetic flow meters were used to measure the flow rates of the test solution, cooling water, tube-side streams, and shell-side streams. According to the manufacturer specifications, the accuracy of the flow rate measurements is ± 0.5%. A motor speed controller for the recirculating pump was used to control the flow rate of the test solution. In the static mixer experiments, the tested flow rates ranged from 0.80 gpm to 4.00 gpm.

The run order of the experiments was randomized with respect to flow rate. Rod and position were also randomized for one of the experiments, but this led to more frequent damage to the blades on the static mixers. As such, it was determined to be impractical to continue randomizing the rods and positions.

3.2 Static mixer design

Four 48-inch carbon fiber rods were used as static mixers. Small holes were drilled on each rod. These were evenly spaced three inches apart to allow attachment of the three-dimensional printed blades, which were attached with epoxy. Then, the blades were coated with superglue to make them water-resistant and prevent fluid from entering the rods. The four static mixer designs are summarized in Table 3.1.

Table 3.1: Static mixer designs.

Rod	Number of blades	Position of blades
1	1	N/A
2	2	1/4, 3/4
3	2	1/3, 2/3
4	3	N/A

Rod 1 had one blade attached near the beginning of the rod. Rods 2 and 3 had two blades each. If fully inserted in the concentric tube heat exchanger, the blades on Rod 2 were spaced one-quarter and three-fourth of the way of the tube. The blades on the latter rod were spaced one-third and two-third of the way of the tube. Rod 4 had 3 blades spaced evenly along the tube when fully inserted. The carbon fiber rods with varying number and spacing of blades were installed into the concentric tube

heat exchanger of the recirculating flow system at various positions. They did not rotate in the heat exchanger, which would otherwise render the static mixer useless.

3.3 Preparation of drag reducing solutions

In all experiments, the test volume was 10 L. The materials used include distilled water, Ethoquad O/12, and sodium salicylate (NaSal). The amount of material varied based on the target mole ratio of counterion to surfactant. The cationic surfactant, Ethoquad O/12, was selected because its drag reducing properties have been well-studied. The stock solution was supplied by Akzo Nobel Chemicals, Inc. It is 75% w/w active in isopropanol with an average molecular weight of 403 g/mol. The structure of Ethoquad O/12 is shown in Figure 3.2.

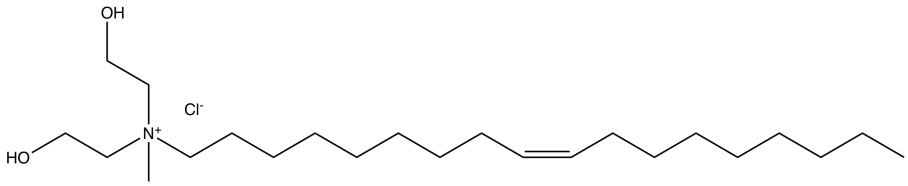

Figure 3.2: Chemical structure of Ethoquad O/12.

Dry chemicals included NaSal, which was purchased from Fisher. It was selected for use as the counterion because it has been widely studied in the context of DR. Also, NaSal has the ability to bind to micelles [5]. The chemical structure of NaSal is shown in Figure 3.3.

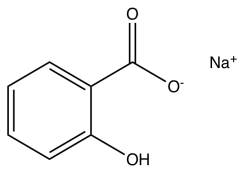

Figure 3.3: Chemical structure of NaSal.

The performance and efficiency of the static mixers were studied using a 5 mM solution of Ethoquad O/12 with 12.5 mM NaSal and a 2.5 mM solution of Ethoquad O/12 with 6.25 mM NaSal. These are summarized in Table 3.2.

Table 3.2: Concentration of test solutions.

Volume (L)	Counterion	Surfactant	Counterion to surfactant ratio	Concentration of surfactant (mM)
10	Sodium salicylate	Ethoquad O/12	2.5:1	5
10	Sodium salicylate	Ethoquad O/12	2.5:1	2.5

The surfactant DR solutions were made with the following procedure. Below is an example for 10 L of 5 mM Ethoquad O/12 with 12.5 mM NaSal.

1. Calculate the amount of surfactant required.

   A. Multiply the desired volume by the molarity of the surfactant.

$$10\ L * 0.005\ \frac{mol}{L} = 0.05\ mol \tag{3.1}$$

   B. Multiply mole by the desired surfactant's molecular weight.

$$0.05\ mol * 403\ \frac{g_{surfactant}}{mol} = 20.15\ g_{surfactant} \tag{3.2}$$

C. Divide by weight fraction of surfactant in stock solution.

$$\frac{20.15\ g_{surfactant}}{0.75\frac{g_{surfactant}}{g_{stock}}} = 28.87\ g_{stock} \tag{3.3}$$

2. Calculate the amount of counterion required.

A. Multiply the moles of surfactant by the counterion ratio.

$$0.05\ mol_{surfactant} * 2.5\frac{mol_{counterion}}{mol_{surfactant}} = 0.155\ mol_{counterion} \tag{3.4}$$

B. Multiply by the molecular weight of the counterion.

$$0.155\ mol_{counterion} * 160.11\ \frac{g_{counterion}}{mol_{counterion}} = 20.15\ g_{counterion} \tag{3.5}$$

3. Pour approximately 25 g Ethoquad O/12 into a 100 mL beaker.

4. Weigh out the desired amount of sodium salicylate.

5. Tare an empty 100 mL beaker.

6. Using a plastic pipette, draw 1/5 of the Ethoquad O/12 necessary into the empty beaker.

7. Fill a 500 mL Erlenmeyer flask with 500 mL distilled water.

8. Pour a small amount of the distilled water from the Erlenmeyer flask into the beaker from Step 5. Stir with a glass thermometer to get as much of the surfactant into solution.

9. Pour this into a 4 L Nalgene beaker. Stir aggressively with the thermometer.

10. Continue pouring the distilled water into the beaker then into the 4 L Nalgene beaker to get as much of the surfactant as possible. Repeat Steps 7-9 until 2 L are made up.

11. Add approximately 1/5 of the sodium salicylate required to the 4 L beaker and stir aggressively.

12. Carefully pour the 2 L solution from the 4 L beaker into a 5 gal container.

13. Repeat Steps 6-12 until 10 L of solution are made up.

14. Let the solution equilibriate for at least 24 hrs before testing.

3.4 Drag reduction measurements

DR is defined as the percent reduction of the friction factor relative to that of the solvent at the same flow rate and temperature conditions. DR% generally increases with increasing solvent Reynolds number and can approach 90% in surfactant solutions [5]. This can be calculated with the equation

$$DR\% = \frac{f_{water} - f}{f_{water}} * 100\%, \tag{3.6}$$

where f_{water} and f are the friction factors of the solvent and drag reducing solution, respectively. DR was measured at a fixed solvent Reynolds number, which was changed by adjusting the flow rate of the test solution. The friction factor for water is calculated with the Prandtl-Karman equation

$$\frac{1}{\sqrt{f}} = 4log_{10}(Re\sqrt{f}) - 0.4, \tag{3.7}$$

where f is the Fanning friction factor, and Re is the Reynolds number. Re is given by

$$Re = \frac{\rho v D}{\mu}, \tag{3.8}$$

where ρ is the density of the fluid, v is the velocity of the fluid, D is the diameter of the pipe, and μ is dynamic viscosity of the fluid. The Fanning friction factor of the drag reducing solution at the same flow rate is calculated using the equation

$$f = \frac{\tau}{\rho\frac{v^2}{2}}, \tag{3.9}$$

where τ is wall shear stress, ρ is the density of the fluid (solvent), and v is the bulk flow velocity. The local shear stress, τ, is given by the equation

$$\tau = \frac{\Delta P D}{4L}, \tag{3.10}$$

where ΔP is the pressure drop, D is the diameter of the pipe, and L is the length of the pressure drop section. The pressure drop is determined with measurements by the differential pressure transducers. D and L are known system parameters.

3.5 Heat transfer reduction measurements

HTR is defined as the percent reduction of the Nusselt number relative to that of the solvent at the same flow rate and temperature conditions. This is given by the equation

$$HTR\% = \frac{Nu_{water} - Nu}{Nu_{water}} * 100\%, \tag{3.11}$$

where Nu_{water} and Nu are the Nusselt numbers of the solvent and drag reducing solution, respectively. The Nusselt number an be calculated with the equation

$$Nu = \frac{hD}{k}, \tag{3.12}$$

where h is the convective heat transfer coefficient, D is the diameter of the pipe, and k is the thermal conductivity of the fluid. Using the thermophysical properties of water, HTR% can be simplified to

$$HTR\% = \frac{h_{water} - h}{h_{water}} * 100\%, \tag{3.13}$$

where h_{water} and h are the convective heat transfer coefficients of the solvent and drag reducing solution, respectively. The tube diameter and thermal conductivity were assumed to be the same for both the drag reducing solution and the solvent, so HTR% could be calculated as the percent reduction in the heat transfer coefficient relative to that of the solvent.

Chapter 4: Results and Discussion

4.1 Half concentration experiment

The static mixer experiments were run using a total surfactant concentration of 2.5 mM Ethoquad O/12 with a counterion to surfactant ratio of 2.5:1. DR, HTR, and pressure drop data were collected and compared.

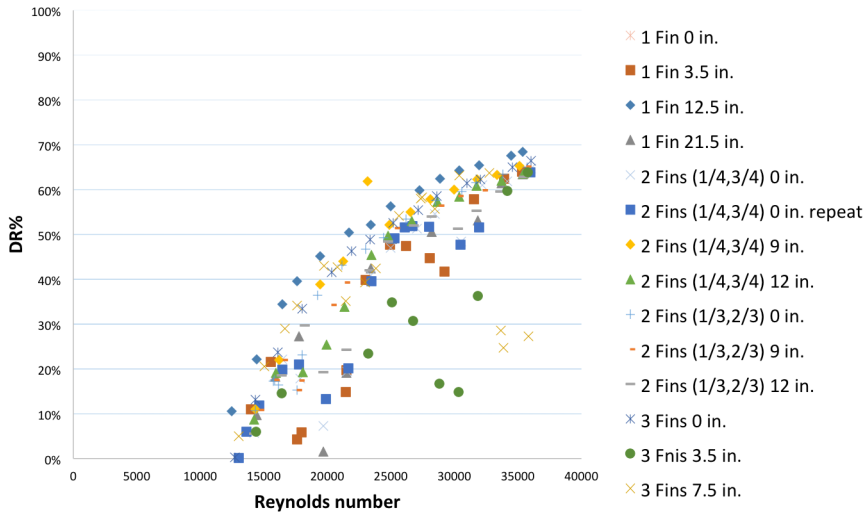

Figure 4.1: DR% vs. Reynolds number for 6.25 mM NaSal:2.5 mM Ethoquad O/12 solution with Rods 1-4 in all tested positions.

The number of blades and the position of the rods in the heat exchanger tube did not have significant effects on the DR of the solution. As shown in Figure 4.1, the DR% was similar for the four rods in all experiments. There is some unexpected DR behavior observed, which can be explained by aging of the solution.

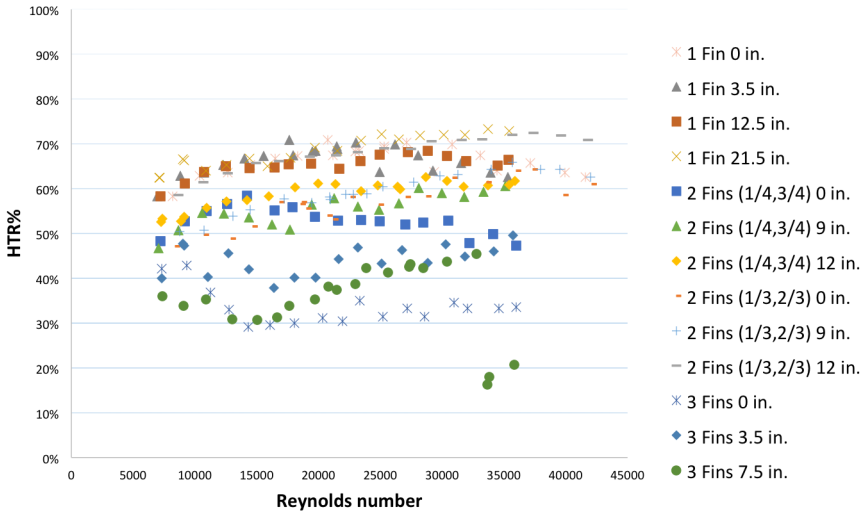

Figure 4.2: HTR% vs. Reynolds number for 6.25 mM NaSal:2.5 mM Ethoquad O/12 solution with all Rods 1-4 in all tested positions.

All the HTR data for the experiments at half concentration are shown in Figure 4.2. The graph allows for direct comparison of all the rods at all positions. The static mixers significantly reduced the HTR from that of the baseline. The position of the static mixers does not appear to affect the HTR as much as the number of blades does. As a general trend, HTR decreases with the addition of a blade. As expected, Rod 4 has the lowest HTR, followed by Rods 2 and 3. Rod 1 has the highest HTR.

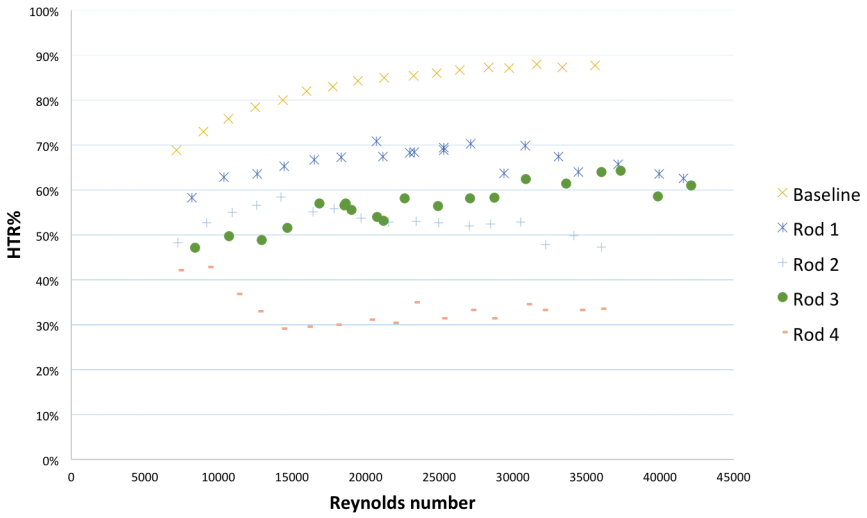

Figure 4.3: HTR% vs. Reynolds number for 6.25 mM NaSal:2.5 mM Ethoquad O/12 solution with Rods 1-4 in the fully inserted position.

This trend is shown more clearly in Figure 4.3. The baseline has an HTR of 90%. Adding one blade with Rod 1 decreases the HTR from 90% to 70%. Rods 2 and 3 have similar HTR in the 50-65% range, and Rod 4 has the lowest HTR of 30%.

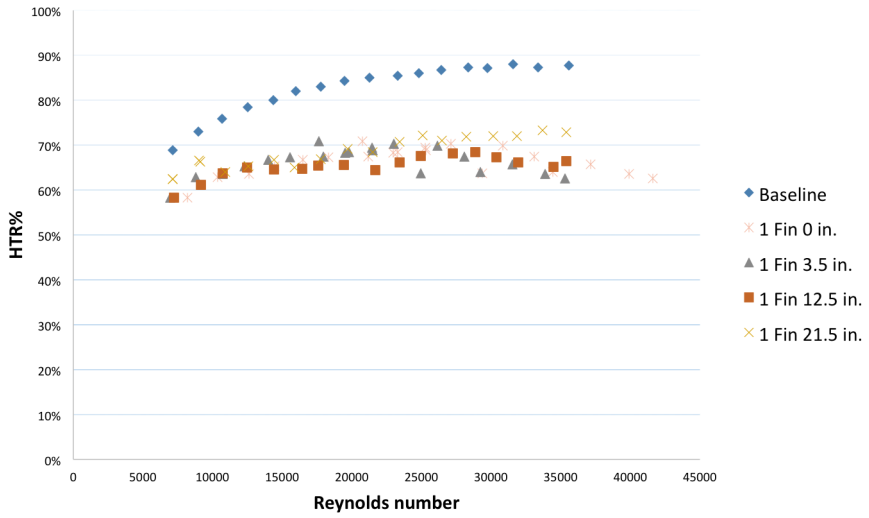

Figure 4.4: HTR% vs. Reynolds number for 6.25 mM NaSal:2.5 mM Ethoquad O/12 solution with Rod 1 in all tested positions.

The HTR data for Rod 1 at all tested positions are represented in Figure 4.4. Compared with the baseline, the addition of one blade reduced the HTR from 90% to 70%. The position of the rod does not appear to affect the HTR of this rod, as the HTR is relatively similar for all tested positions. The graph shows significant overlap with the four curves.

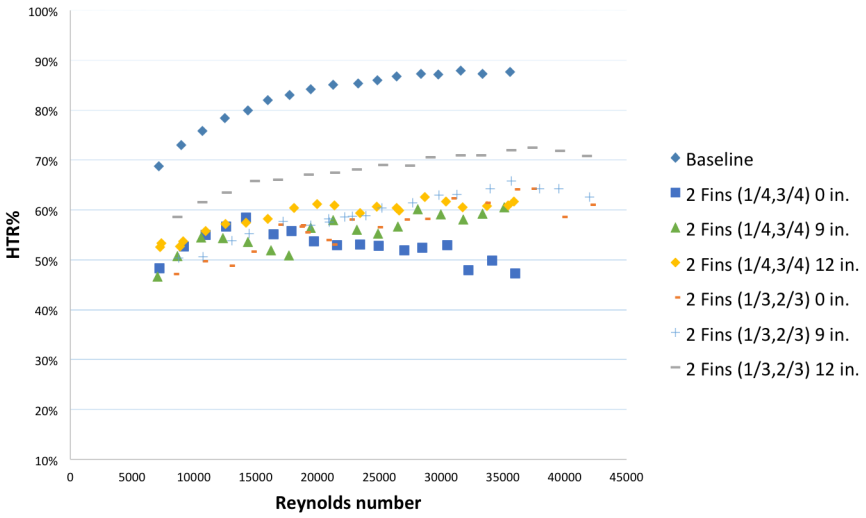

Figure 4.5: HTR% vs. Reynolds number for 6.25 mM NaSal:2.5 mM Ethoquad O/12 solution with Rods 2 and 3 in all tested positions.

The HTR data for Rods 2 and 3 at all tested positions are represented in Figure 4.5. Similar to the observations made with Rod 1, the position of Rods 2 and 3 does not appear to affect the HTR. With two blades, the HTR is relatively similar for all tested positions for both rods. Some variation in the data can be attributed to the aging of the solution.

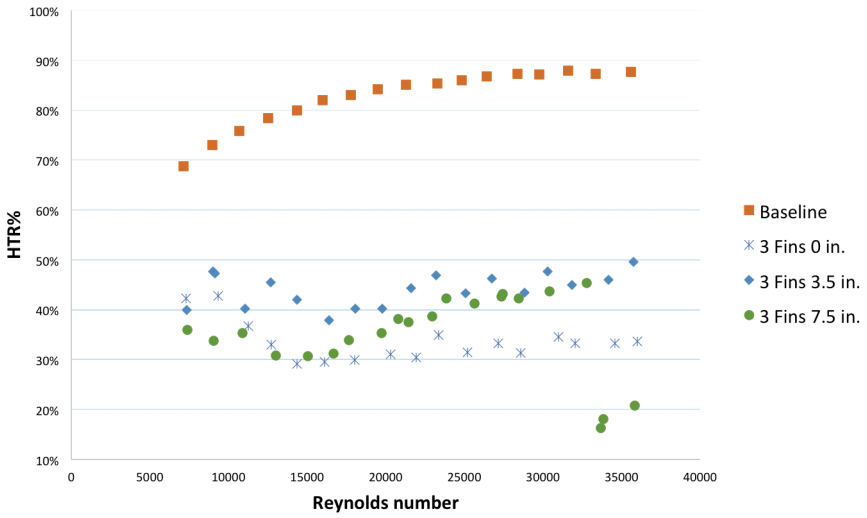

Figure 4.6: HTR% vs. Reynolds number for 6.25 mM NaSal:2.5 mM Ethoquad O/12 solution with Rod 4 in all tested positions.

The HTR data for Rod 4 at all tested positions are shown in Figure 4.6. Here, it is also determined the position of the rod in the heat exchanger tube does not have a significant effect on the HTR. With the 7.5 inch position, three data points experience extremely lower HTR than the rest of the data set. This can be explained by the aging of the DR solution, as this test was run a few days after the other two positions were tested. At higher solvent Reynolds number, the high flow rates and exposure to shear causes the DR solution to exhibit heat transfer coefficients similar to those of water.

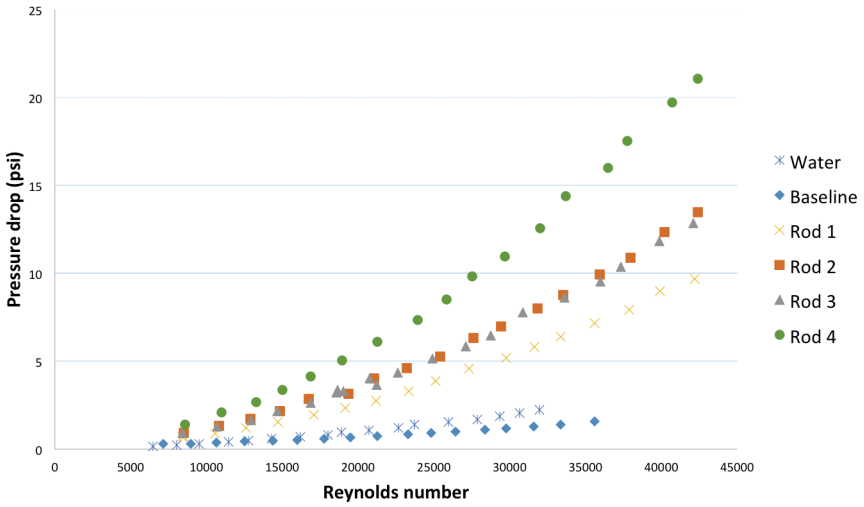

Figure 4.7: Pressure drop vs. Reynolds number for 6.25 mM NaSal:2.5 mM Ethoquad O/12 solution with Rods 1-4 in the fully inserted position.

The pressure drop data for all four rods in the fully inserted position are compared with each other, water, and the baseline in Figure 4.7. As expected, the baseline DR solution has a lower pressure drop than that of water. With the addition of a rod and with increasing number of blades, the pressure drop increases linearly. Rod 4 has the highest pressure, followed by Rods 2 and 3. Rod 1 has the lowest pressure drop. Rods 2 and 3 both have two blades, and their pressure drop penalties are not significantly different.

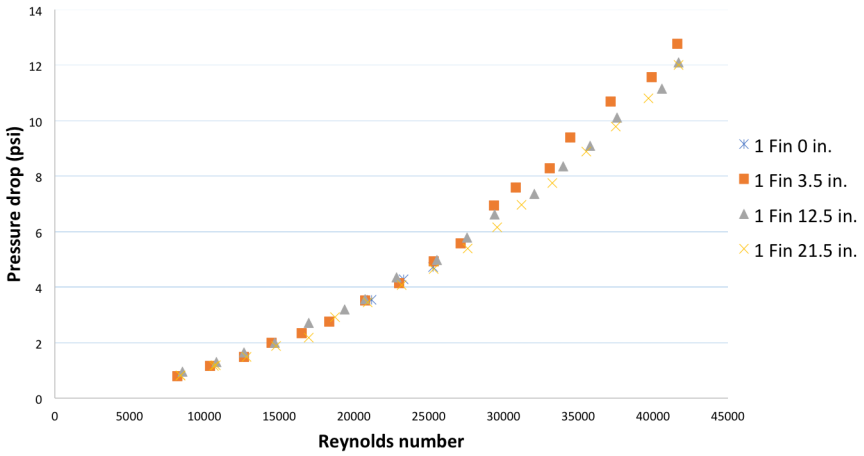

Figure 4.8: Pressure drop vs. Reynolds number for 6.25 mM NaSal:2.5 mM Ethoquad O/12 solution with Rod 1 in all tested positions.

The pressure drop data for Rod 1 are shown in Figure 4.8. The position of this rod in the heat exchanger tube does not have a significant effect on the pressure drop. The graph shows major overlap with the four curves.

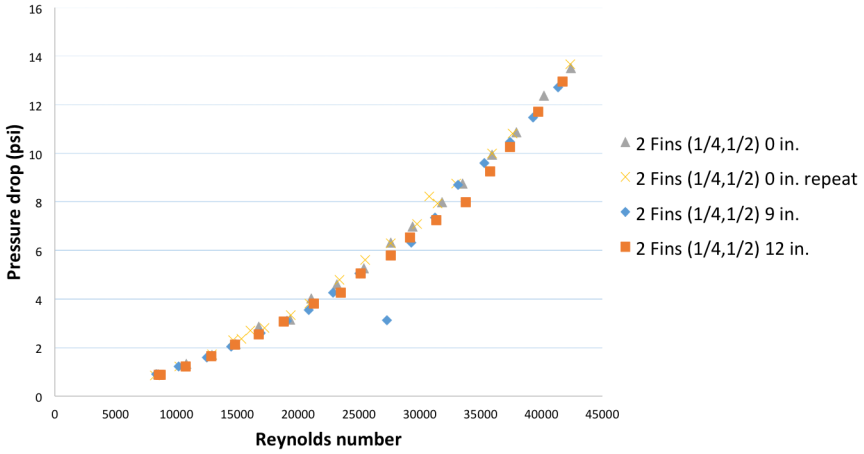

Figure 4.9: Pressure drop vs. Reynolds number for 6.25 mM NaSal:2.5 mM Ethoquad O/12 solution with Rod 2 in all tested positions.

Similar to observations made with Rod 1, varying the position of Rod 2 does not have a significant effect on the pressure drop data. This is represented graphically in Figure 4.9. The four curves show significant overlap.

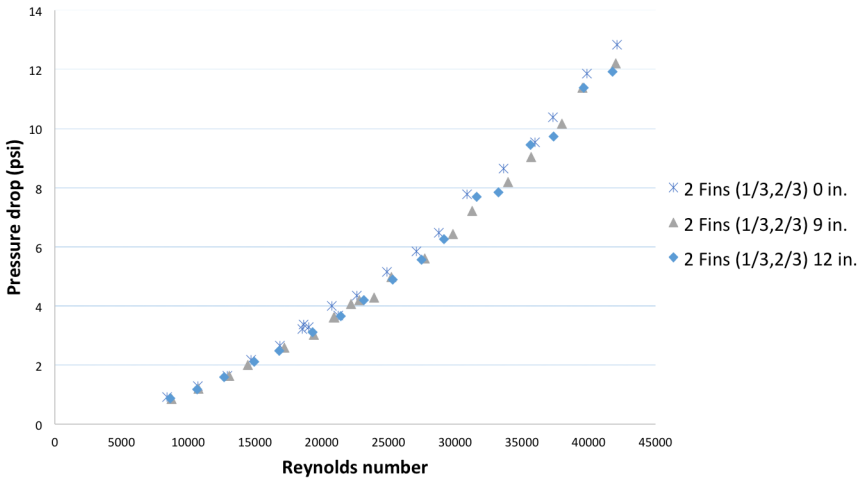

Figure 4.10: Pressure drop vs. Reynolds number for 6.25 mM NaSal:2.5 mM Ethoquad O/12 solution with Rod 3 in all tested positions.

The pressure drop data for Rod 3 is shown in Figure 4.10. Changing the position of the rod does not have a significant effect on the pressure drop. As expected, these data are not significantly different than those of Rod 2.

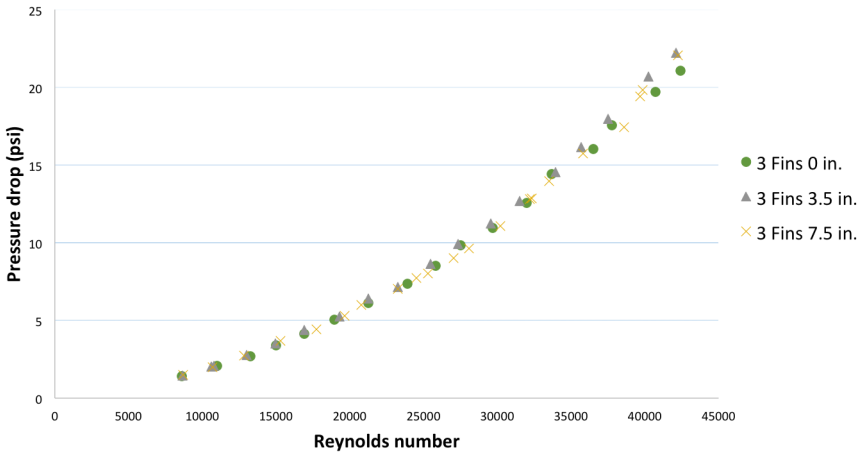

Figure 4.11: Pressure drop vs. Reynolds number for 6.25 mM NaSal:2.5 mM Ethoquad O/12 solution with Rod 4 in all tested positions.

The pressure drop data for Rod 4 is shown in Figure 4.11. Similar to the analysis of the previous three rods, the position of Rod 4 in the heat exchanger tube does not have a significant effect on the pressure drop. The graph shows major overlap with the three curves.

4.2 Full concentration experiment

The static mixer experiments were repeated using a total surfactant concentration of 5 mM Ethoquad O/12 with a counterion to surfactant ratio of 2.5:1. DR, HTR, and pressure drop data were collected and compared. Results from experiments with the full concentration solution are similar to those gathered with half the concentration. As such, many graphs are omitted.

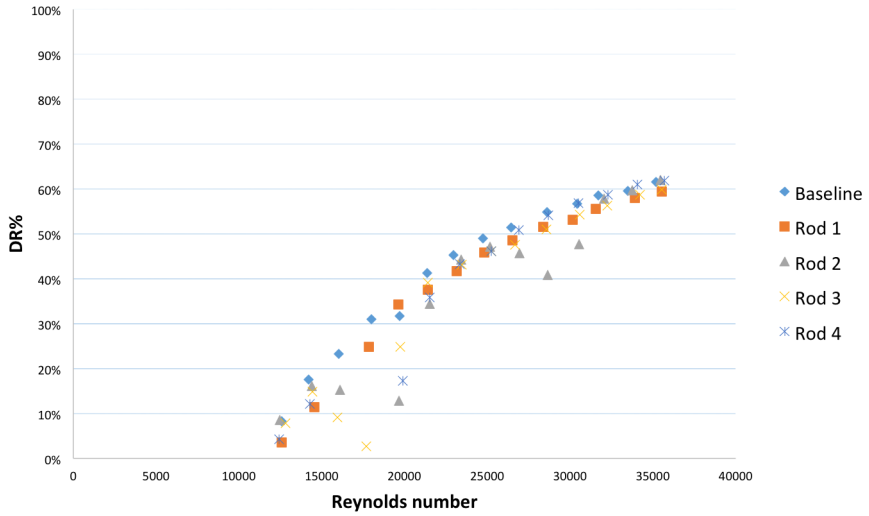

Figure 4.12: DR% vs. Reynolds number for 12.5 mM NaSal:5 mM Ethoquad O/12 solution with Rods 1-4 in the fully inserted position.

DR data for Rods 1 through 4 in the fully inserted position are compared with each other and with the baseline in Figure 4.12. All 5 curves overlap and follow a similar trend: as Reynolds number increases, the DR increases. The different static mixer designs do not have a significant effect on the DR. Although not shown here, the position of the rods did not significantly affect the DR either.

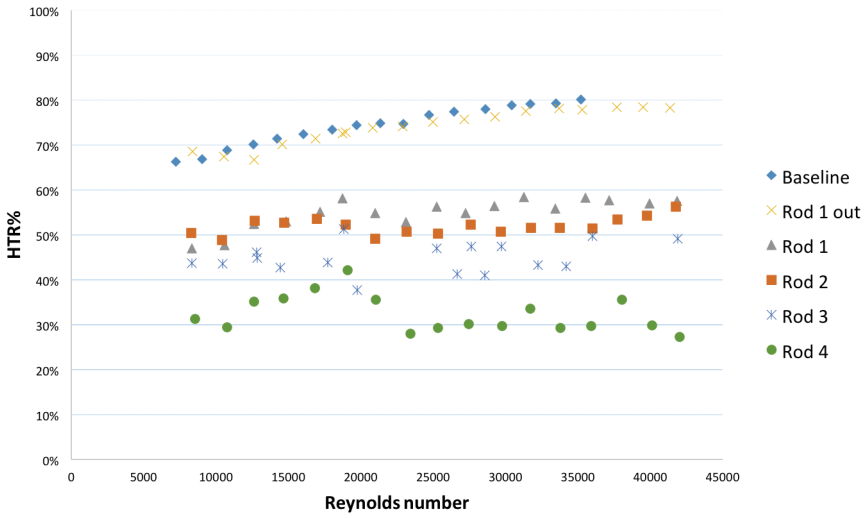

Figure 4.13: HTR% vs. Reynolds number for 12.5 mM NaSal:5 mM Ethoquad O/12 solution with Rods 1-4 in the fully inserted position and Rod 1 pulled out of the heat exchanger.

HTR data for Rods 1 through 4 in the fully inserted position are compared with each other and with the baseline in Figure 4.13. The yellow markers represent Rod 1 when pulled out of the heat exchanger tube. This exhibits HTR very close to that of the baseline. This is expected, as the blade is not in the heat exchanger to disrupt the thermal boundary layer and enhance heat transfer. With the addition of each blade, the HTR decreases. Installing Rod 1 with the single blade significantly reduces the HTR from 80% to 60%. Rods 2 and 3 have similar HTR around 50%, and Rod 4 has the lowest HTR of 30%. As expected, more blades are able to impart more bulk mixing in the heat exchanger to enhance heat transfer. Although not shown here, the position of each rod did not have a significant effect on HTR.

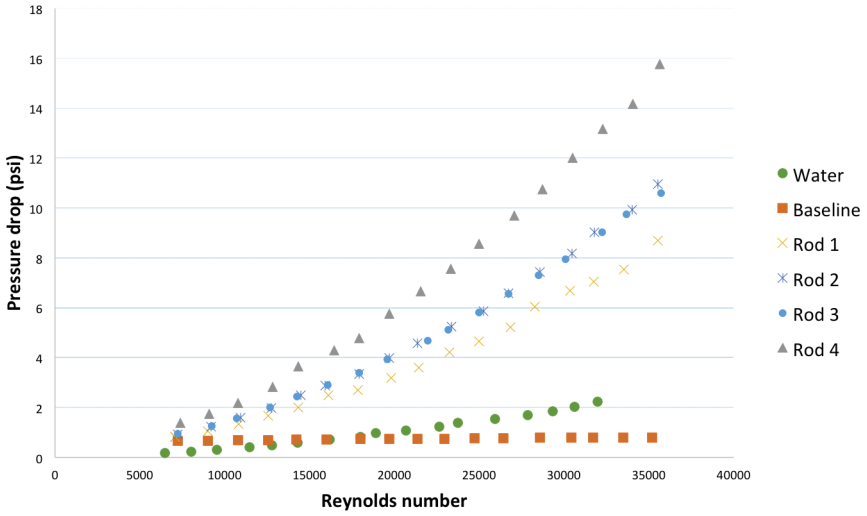

Figure 4.14: Pressure drop vs. Reynolds number for 12.5 mM NaSal:5 mM Ethoquad O/12 solution with Rods 1-4 in the fully inserted position and Rod 1 pulled out of the heat exchanger.

In Figure 4.14, the pressure drop of water is shown with green circles. As expected, the pressure drop of the baseline is lower than that of water. This is what gives DR solutions the pumping energy savings. With the introduction of the static mixers and increasing number of blades, the pressure drop increases. Rod 4 has the largest pressure drop, followed by Rods 2 and 3. Rod 1 has the lowest pressure drop.

4.3 Hollow blade design

Although the HTR is significantly reduced with each additional blade, the pressure drop is simultaneously increased. To minimize the pressure loss in the system, a hollow blade design was tested for a single fin rod. The blade was carved out in the center to allow the fluid to pass through.

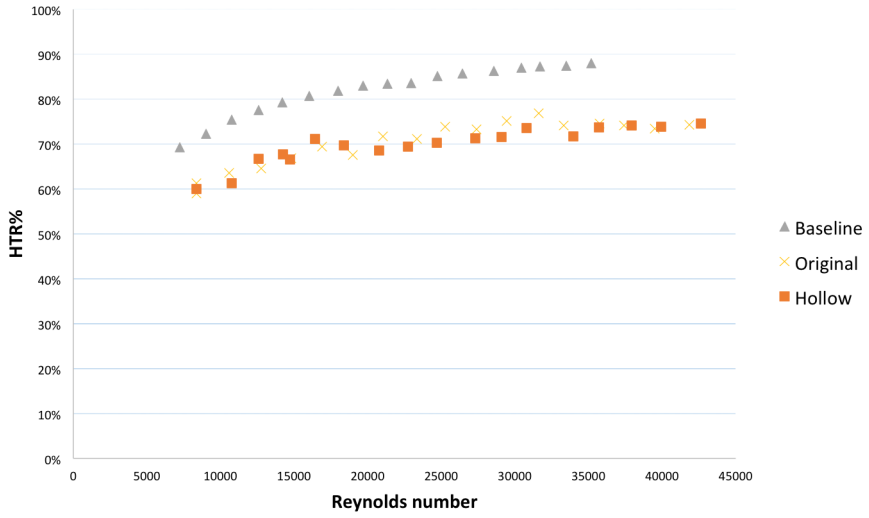

Figure 4.15: Comparing the HTR of the original and hollow designs for the 12.5 mM NaSal:5 mM Ethoquad O/12 solution.

As shown in Figure 4.15, the HTR with the original one blade design is significantly reduced compared with that of the baseline. With the improved hollow design, the HTR is not significantly affected. The curves of the original and hollow designs overlap.

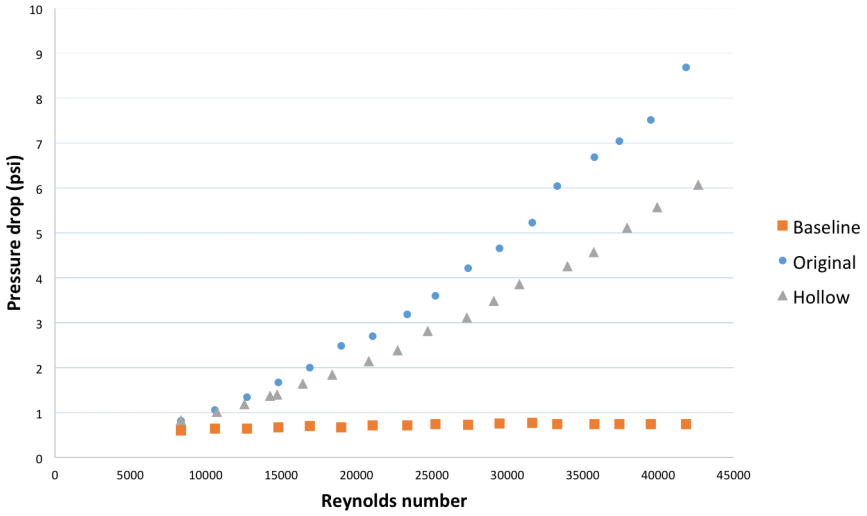

Figure 4.16: Comparing the pressure drop of the original and hollow designs for the 12.5 mM NaSal:5 mM Ethoquad O/12 solution.

The pressure drop data for the baseline, original design, and hollow design are shown in Figure 4.16. The original, single fin rod greatly increases the pressure drop, which is undesirable. After implementing the hollow design, the pressure drop is shown to be reduced.

4.4 Statistical analysis

Data from the static mixer experiments were analyzed with JMP statistical software. All analyses were performed using a significance level of 0.05. An analysis of variance (ANOVA) test was performed for each static mixer design and position at both concentrations of the surfactant DR solution. Ordered differences reports were generated by comparing means with the All Pairs, Tukey HSD test. These reports were used to assess the effects of the different levels of Rod and Number of Blades on HTR and pressure drop.

In all experiments, it was determined the number of blades had a significant effect on HTR for all rods, except Rods 2 and 3. This is expected because Rods 2 and 3 both have two blades. The p-values when comparing all levels were less than 0.001, except when comparing Rods 2 and 3. As predicted, the pressure drop increased linearly with increasing number of blades. At both concentrations, the different static mixer designs and varying positions in the heat exchanger did not have significant effects on DR.

A predictive model, which is shown in Equation 4.1, was developed with JMP with a Fit Y by X of HTR by Number of Blades. This prediction expression was used to predict the number of blades this system would require to reduce HTR to 0%, which is six blades evenly spaced.

$$\text{HTR} = 0.5282166 + \text{Match}(\text{Number of Blades}) \begin{cases} \text{"0"} & \Rightarrow 0.21468940313235 \\ \text{"1"} & \Rightarrow 0.06240746995588 \\ \text{"2"} & \Rightarrow -0.0722861493971 \\ \text{"3"} & \Rightarrow -0.2048107236912 \\ else & \Rightarrow \end{cases} \quad (4.1)$$

4.5 Data reduction

Maxson developed a parameter to evaluate the heat transfer enhancement efficiency called the enhancement efficiency factor, p [5]. This allows for a quick assessment of the improvement in heat transfer at a specific Reynolds number and is given by

$$p = \frac{HTR_{without\ device} - HTR_{with\ device}}{power\ \ consumption}, \tag{4.2}$$

where power consumption can be calculated by multiplying the pressure drop across the heat exchanger and the volumetric flow rate.

The enhancement efficiency factors for the full concentration experiment are shown in Figure 4.17. Rods 1 through 4 had high efficiency at lower Reynolds numbers. At higher Reynolds numbers, the efficiency is observed to converge to a similar, lower p.

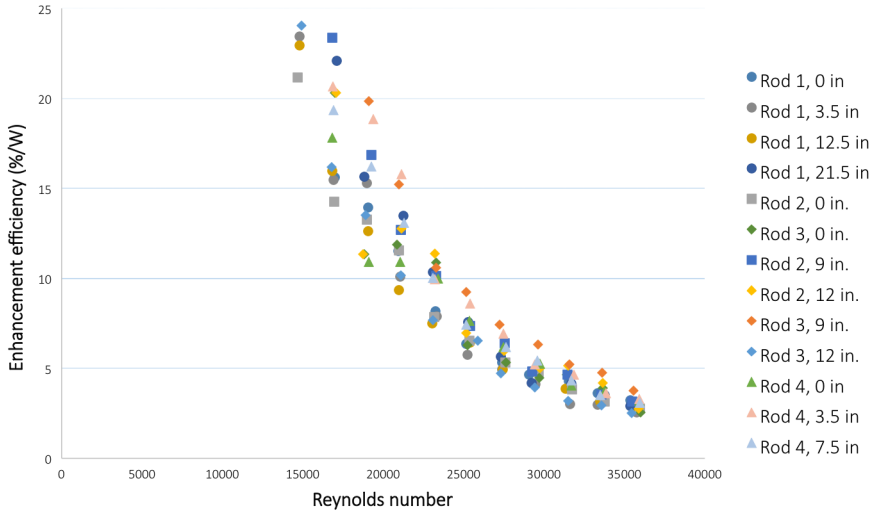

Figure 4.17: Comparison of the enhancement efficiency factor, p, for Rods 1-4 at all tested positions.

4.6 Conclusions

Adding a static mixer and increasing the number of blades significantly enhanced the heat transfer ability of the 2.5 mM and 5 mM Ethoquad O/12 solutions. Compared with Rods 1 through 3, Rod 4 had the highest improvement to heat transfer. With Rod 4, HTR reached as low as 30%. Rods 2 and 3 had comparable effects, as they both had two blades each.

This improvement in heat transfer was coupled with larger pressure drop penalties as high as 25 times that of water or the baseline. To minimize the pressure drop caused by the increased number of blades on the static mixers, a hollow blade design was implemented. Compared with the original blades, the hollow blade did not significantly affect DR or HTR, but it did decrease the pressure drop.

With respect to heat transfer, the core of the flow is relatively insignificant compared to the edges. The hollow blade designs were able to disrupt the thermal boundary layer on the conduit walls, so bulk mixing was still achieved to enhance heat transfer.

Using the enhancement efficiency factor as reference, the static mixers were observed to have high heat transfer enhancement efficiency at lower Reynolds numbers.

Chapter 5: Contributions and Future Work

5.1 Future work

Due to time constraints, many designs, tests, and experiments have been left for the future. This thesis mainly focused on testing the four static mixer designs to identify the optimal configuration and position, which was accomplished. It was determined the rod with three blades in the fully inserted position had the lowest HTR. Results from the experiments suggested potential adjustments to the static mixer designs to improve the heat transfer while minimizing the pressure drop penalty. The following ideas can be explored:

1. The predictive model constructed with JMP suggested six blades would reduce HTR% to 0%. A carbon fiber rod can be made with 6 blades evenly spaced and tested to validate the model. If the model is determined to be accurate, more work can be done to scale up the static mixer.

2. The hollow blade design can be further investigated. A new blade design with struts for support can be made with SolidWorks and 3-D printed for use in future experiments.

3. The direction of blades could also be changed. The blades could alternate to face each other.

4. It could be interesting to explore the effect of changing the pitch from 45 degrees to 30 degrees. This would require lengthening the blades to fit the diameter of the tube.

Bibliography

[1] G.G. Aguilar, K.K. Gasljevic, and E.F. Matthys. "Coupling Between Heat and Momentum Transfer Mechanisms for Drag-Reducing Polymer and Surfactant Solutions". *ASME Journal of Heat Transfer*, 121(4):796–802, 1999.

[2] Kim C.A., J.T. Kim, K. Lee, H.J. Choi, and Jhon M.S. "Mechanical degradation of dilute polymer solutions under turbulent flow". *JPolymer*, 41(21):7611–7615, 2000.

[3] Z. Chara, J.L. Zakin, and M. Severa. "Turbulence measurements of drag reducing surfactant system". *Experiments in Fluids*, 16(1):36–41, 1993.

[4] A. Lake, B. Rezaie, and S. Beyerlein. "Review of district heating and cooling systems for a sustainable future". *Renewable and Sustainable Energy Reviews*, 67:417–425, 2017.

[5] A.J. Maxson. *Heat Transfer Enhancement in Turbulent Drag Reducing Surfactant Solutions*. PhD thesis, The Ohio State University, 2017.

[6] Y. Qi, Y. Kawaguchi, R. Christensen, and J.L. Zakin. "Enhancing heat transfer ability of drag reducing surfactant solutions with static mixers and honeycombs". *International Journal of Heat and Mass Transfer*, 46(26):5161–5173, 2003.

[7] Castro W. and Squire W. "The effect of polymer additives on transition in pipe flow". *Applied Scientific Research*, 18(1):81–96, 1968.

[8] Y. Wang, B. Yu, J.L. Zakin, and H. Shi. "Review on Drag Reduction and Its Heat Transfer by Additives". *Advances in Mechanical Engineering*, 3:478–479, 2011.

[9] Jinjia Wei, Yasuo Kawaguchi, and Bo Yu. *Drag Reduction of Turbulent Flow by Additives*. Hindawi Publishing Corporation, 2011.

[10] Kawaguchi Y., Li F.C., Yu B., and Wei J.J. "Turbulent Drag Reduction with Surfactant Additives Basic Research and Application to an Air Conditioning System". *New Trends in Fluid Mechanics Research*, pages 29–36, 2007.